

# Surface Acoustic Wave Devices for Wireless Strain Measurement

T.-L. Chin<sup>a</sup>, Peng Zheng<sup>b</sup>, Irving J. Oppenheim<sup>c,d\*</sup>, David W. Greve<sup>c,e</sup>

<sup>a</sup> Ph.D. Candidate, Electrical and Computer Eng., Carnegie Mellon University, Pittsburgh, PA 15213

<sup>b</sup> Ph.D. Candidate, Physics, Carnegie Mellon University, Pittsburgh, PA 15213

<sup>c</sup> Faculty Fellow, National Energy Technology Laboratory

<sup>d</sup> Professor, Civil and Environmental Eng., Carnegie Mellon University, Pittsburgh, PA 15213

<sup>e</sup> Professor, Electrical and Computer Eng., Carnegie Mellon University, Pittsburgh, PA 15213

## ABSTRACT

Strain monitoring is a nondestructive inspection method that can reveal the redistribution of internal forces, or the presence of anomalous loadings, in structures. Surface acoustic wave (SAW) devices are small, robust, inexpensive solid-state components in which a wave propagates along the surface of a piezoelectric material, and such devices are used in large numbers commercially as delay devices and as filters. Changes in strain or temperature cause shifts in the acoustic wave speed, by which such SAW devices can also serve as sensors. We present analytical, FEM simulation, and experimental studies on SAW devices fabricated in our laboratory on lithium niobate wafers, with an inter-electrode spacing of 8 micrometers. We discuss the change in wave speed with temperature and with strain, we outline the influence of rotated cuts for the piezoelectric substrate, and we show results of laboratory sensing experiments. Moreover, an electrode on a SAW device can be terminated as an antenna and interrogated with a wireless RF probe to act as a passively-powered device, and we present laboratory results incorporating such wireless performance in our research investigation. We pattern one set of electrodes on the SAW device as a transducer connected to the antenna, and other sets of electrodes on the device acting as reflectors of the surface acoustic wave. At the RF frequencies used for SAW devices, it is realistic to use directional antennas on the probe unit to achieve reasonable stand-off distances.

**Keywords:** Piezoelectric, strain sensing, surface acoustic wave, wireless.

## 1. INTRODUCTION

A significant proportion of structural collapses are preceded by changes in the state of a structure that could be identified by an experienced engineer, if appropriate measurements (observations, sensor data) are provided. While some failure mechanisms will fall outside of this category, a significant number of collapses (or damage conditions that force the infrastructure system to be removed from service) can be intercepted. For example, collapses are known to have occurred in large transportation or industrial structures under the following circumstances:

- Malfunction of girder expansion joints, transmitting large horizontal forces to support piers sufficient to cause structural cracking with collapse potential.
- Foundation movement in a multi-span system leading to lateral-torsional buckling in continuous girders.
- Shrinkage effects inducing unrelieved tension forces leading to connection failure.

A common element in these failures is the appearance of an anomalous force level in one or more members, caused by the redistribution of load or by (unexpected) self-induced forces. In retrospect all such failures could have been prevented by choices at the design stage or by scrupulous attention to changing conditions in the field. Nonetheless, improved measurement of force levels in critical members would bring these developing conditions to the engineer, who serves as the equivalent of the physician. We note that critical members are not limited to those which fail, but include other members that would equally be revealing of the anomaly; for example, the force in a column is a measure of the

---

\* Contact author: ijo@cmu.edu; 412-268-2950; Carnegie Mellon University, Department of Civil and Environmental Engineering, Pittsburgh, PA, 15213.

support reaction. To our observation, significant progress toward this goal has been shown by industry participants (mostly based in Europe, exemplified by SMARTEC and OSMOS) installing technologies that measure position, or relative displacement, with high precision using fiber optics. We consider their demonstration projects to be good examples of SHM per the medical analogy. An engineer can review patterns of displacement over time and can recognize anomalies that warrant further analysis.

We believe that periodic measurement of strain on critical members is another candidate for SHM, and that anomalous strain changes should trigger an engineering review. Resistance strain gauges, properly compensated for temperature, are the “gold standard” measurement technology. However, wired installations are undesirable because of the costs involved. Similarly, battery-powered wireless installations are unrealistic for long term use. A solar-powered wireless installation might be practical if one measurement point is of sufficient interest and is favorably positioned, but we envision the need to monitor strain at somewhere between 10 and 100 points in a typical structure. Energy scavenging is a candidate technology to power wireless installations, and has been demonstrated with reasonable effectiveness when rotating machinery or high temperature conditions provide the energy sources, but successful operation of a wireless sensor powered by transient structural loadings does not appear to be possible in the short term. However, RF probing, at distances to 10 m, is a feasible technology to activate and communicate with SAW devices that we are studying to measure structural strain. Such SAW devices can be robust, small, and inexpensive to manufacture in large quantities.

## 2. BACKGROUND: SAW DEVICES AND THEIR DEVELOPMENT AS SENSORS

The plane wave that can exist near the surface of an elastic isotropic half-space is termed the Rayleigh wave, and it can be considered the simplest surface acoustic wave. It is non-dispersive, which means that it travels at constant velocity and that its shape is preserved, and its energy is largely contained within a short distance from the surface, which means that its geometric spreading is an inverse power less than that of bulk waves. We use the more general term “surface acoustic wave” when referring to the same phenomenon in a nonisotropic material. Of particular interest are the surface acoustic waves that can form on piezoelectric wafers, because the wave can be excited by electrodes patterned on the surface of the wafer [12] and its electromechanical behavior can be used as a sensing mechanism.

Reindl [8] shows a striking SEM image of pulse trains propagating on the surface of a piezoelectric wafer. The pulse trains were generated by two closely-spaced groups of electrodes that form an interdigital transducer (IDT). A voltage is applied to the IDT, and because of the piezoelectric property of the material the electric field that forms between the IDT electrodes creates strains (particle displacements) in the solid. The particle displacements are disturbances that propagate as elastic waves, including the surface acoustic wave of interest in this proposed work. The manufacture of SAW devices [5] is a major industry, and they are applied in large numbers as delay lines and filters [4].

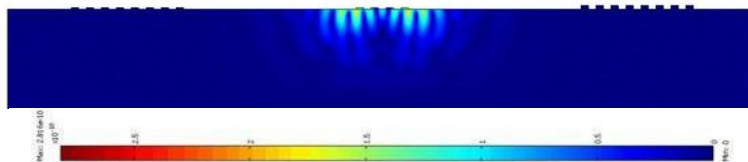


Figure 1. Finite element transient simulation of wave propagation

Figure 1 is a snapshot from a finite element simulation of representative SAW device behavior. It is a COMSOL 2-D model in piezoelectric plane strain, a vertical section through the wafer, in which the surface is the upper boundary. The material is lithium niobate,  $\text{LiNbO}_3$ , in YZ cut;  $\text{LiNbO}_3$  is widely used for SAW devices because of its relatively high electro-acoustic coupling factor. The following features are noted in Figure 1, and are easily recognizable when viewing the results in animation:

- Four electrodes on the surface, at the very center of the image, are the source of the wave, and the excitation is a windowed 5-cycle sinusoidal voltage with a center frequency of 850 MHz. The snapshot was taken at roughly 11 ns, when the centers of the pulse trains have traveled 0.04 mm. (Such an electrode pattern is not suggested

for device operation, but was chosen to produce a simulation that could be easily displayed as snapshots and easily viewed as an animation.)

- The colors in Figure 1 are the total particle displacement at each point. In the animation, or in snapshots at earlier points in time (not shown), bulk waves are plainly visible at the start of the transient response but diminish because of geometric spreading, whereas the surface acoustic wave retains significant energy.
- Two sets of receiving electrodes are incorporated in the model to illustrate their electromechanical interaction with the surface acoustic wave: eight electrodes, 200 nm thick, are located 0.04 mm to the left of center, and eight electrodes 500 nm thick located and 0.04 mm to the right of center. Figure 1 shows the surface acoustic waves arriving at those two electrode locations; it shows scattering from those two sets of receiving electrodes, including the difference introduced by a greater electrode mass at the right.

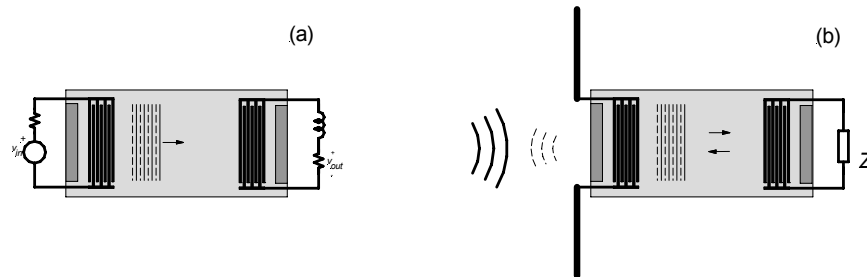


Figure 2. a) Wired SAW device; b) Single antenna RF operation of SAW device

A representative SAW device application is its use as a delay line. Figure 2a shows a conventional wired configuration in which the IDT at the left is excited by an external voltage, a surface acoustic wave propagates to the right, and the receiving IDT at the right connects to a circuit. However, it has also been demonstrated that a SAW device can be configured as an RFID device or as an RF (wireless) requestable platform [9] for a sensor. Figure 2b shows one possible configuration for the latter, in which the IDT is connected to a single antenna and excited by RF, the surface acoustic wave propagates to the right, and the receiving IDT terminates in an external sensor; the load impedance of that sensor alters the scattering by that IDT and therefore the reflected surface acoustic wave that returns to the left, which then creates an inverse excitation of voltage at the antenna. (Other configurations are not shown but can be reviewed in brief. Many feature one or more reflectors, rather than an IDT, at the right of the device. An RFID device can be created by placing reflectors along the path to encode the ID. Similarly, a wireless, passively-powered sensor can be implemented if the quantity to be detected modifies the wave speed.) SAW devices are typically designed to operate in the frequency range between 400 and 2500 MHz. Operation in the GHz region is particularly well suited to wireless, passively-powered (RF) operation because at these high frequencies it is possible to design highly directional antennas; as a result, there can be a substantial distance between the probe electronics and the SAW device [3]. Extensive research and demonstration has been performed in Germany at Siemens Company and numerous other investigators; one prominent example is a wireless tire pressure sensor [6], another is a torque sensor [13], and many others have been reported [8]. These past projects by others establish the feasibility of using the SAW device technology for wireless strain sensing, but development of such a device for application to physical infrastructure remains a new research question.

As another example, Figure 3 shows a schematic concept to extend an existing wireless SAW device pressure sensor design [8] to include temperature compensation. A single antenna and IDT are located at the midpoint of the wafer. The surface acoustic wave initially traveling to the left, where the wafer spans structurally, allows pressure sensing because the structural strain in the piezoelectric material alters the wave speed; the surface acoustic wave initially traveling to the right allows temperature sensing because temperature change alters the wave speed.

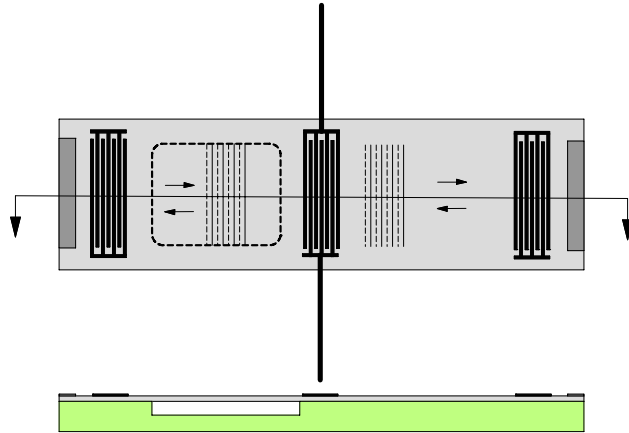


Figure 3. Example for pressure sensing with temperature compensation

Varadan and his coworkers [2] demonstrated wireless operation of SAW devices, which they termed IDTs, for interdigitated transducers, as sensors. Their work included successful development [11] of wireless strain sensors, which they demonstrated to measure dynamic variations in strain under loadings representative of aircraft operation. Our work differs from that earlier work by our use of pulse generation and echo measurement, and our laboratory testing under quasi-static loading.

### 3. DESIGN AND PRELIMINARY TESTING OF A LITHIUM NIOBATE SAW DEVICE

In our recent research activities we designed and fabricated SAW devices on lithium niobate, using a wafer (part number 97-02471-01 from Crystal Technology) in a Y-axis rotated  $128^\circ$  cut, 0.5 mm thick and 100 mm diameter. We designed and fabricated many different device layouts on the wafer, and Figure 4 is a CAD drawing showing one of the layouts employed, showing the device used in our strain sensing test.

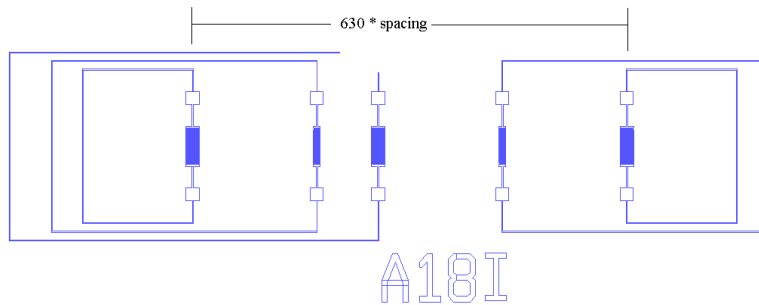


Figure 4. CAD drawing of device layout

This particular device features five IDTs, appearing as the dark rectangles in the image. Each electrode pair features a spacing (or pitch,  $\lambda$ ) of  $8 \mu\text{m}$ , and the electrode length was chosen as  $50\lambda$ . Proceeding left to right, the five IDTs are patterned with 20, 10, 20, 10, and 20 pairs of electrodes, and the center-center spacing between IDTs is  $180\lambda$ ,  $90\lambda$ ,  $180\lambda$ , and  $180\lambda$ . The distance between our source IDT and the most distant reflector is  $630\lambda$ , corresponding to a one-way path length of 5.04 mm. Figure 4 also shows conductors that were patterned to short the two terminals of each IDT to avoid pyroelectric charge accumulation during fabrication. Figure 5 is a microphotograph of another device that we fabricated on the wafer, showing an IDT with 40 pairs of electrodes, with a portion of another IDT at the right of the image.

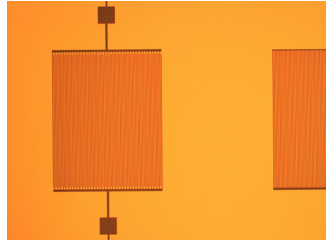


Figure 5. Microphotograph of IDTs on lithium niobate wafer

The pattern of IDTs in Figure 4 will return multiple echoes to the IDT used as the excitation source, and (using a T/R switch) we record those echoes. We conducted experimental measurements to determine the frequency matching the electrode geometry for the device shown in Figure 4 and observed maximum response in this transducer, intended for wired operation, near 440 MHz. Our excitation source is a smoothed squarewave, modulated to 25MHz and upconverted to 440 MHz using a National Instruments PXI-5670 2.7 GHz RF Vector Signal Generator.

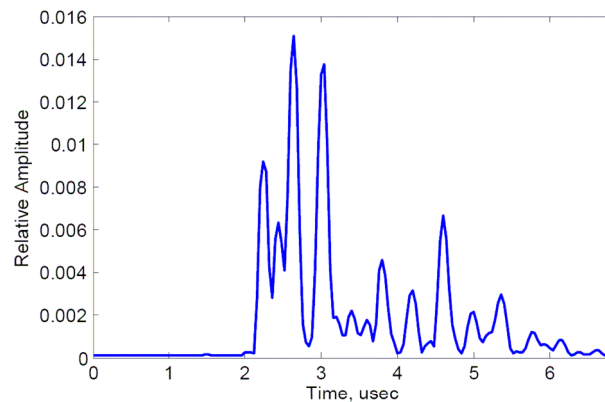


Figure 6. Typical reflections detected (after T/R switching) at excitation source.

Figure 6 shows the multiple echoes returned in a preliminary experiment. The exciting pulse, applied at the IDT at the extreme left in Figure 4, occurs at  $t = 1.86 \mu\text{s}$  and is largely suppressed in magnitude by the T/R switch, which acts from  $1.5 \mu\text{s}$  to  $2.0 \mu\text{s}$ . The arrival near  $4.6 \mu\text{s}$  is the reflection from the most distant IDT, corresponding to a surface acoustic wave speed slightly less than  $3700 \text{ m/s}$ . The prominent peaks near  $2.6 \mu\text{s}$  and  $3.0 \mu\text{s}$  correspond to reflections from IDTs located, respectively,  $180\lambda$  and  $270\lambda$  from the source IDT.

#### 4. STRAIN MEASUREMENT WITH A SAW DEVICE

The device sketched in Figure 4 was mounted on a ceramic DIP package and attached with epoxy to a stainless steel specimen of rectangular cross-section. Figure 7 is a sketch of the test setup, where the specimen is loaded as a cantilever beam by a concentrated load,  $F$ , near its tip. The bending moment is predicted directly by statics, and assumptions of linear elasticity provide the conventional prediction of strain through the thickness of the cross-section. We applied dead load by suspending masses of 1, 2, and 3 kg from the load point. Figure 7 records the material properties and dimensions from which strain can be calculated.

We conducted experiments and measured the phase difference between two echoes with a difference in path length of  $1260\lambda$ . We use IQ phase demodulation to calculate the phase by taking the  $\tan^{-1}(Q/I)$  with a National Instruments PXI-5661 2.7 GHz RF Vector Signal Analyzer with digital downconversion. Our results were obtained averaging 100 points; the standard deviation (across those 100 measurements) of the phase difference is about 0.03 radians, exclusive of constant drift which is also present, and our test results are shown in Figure 8. The phase difference is measured in

radians, and division by  $2\pi$  converts that quantity into a fraction of a wavelength. Division by 1260 (the number of wavelengths in the path difference) then constitutes a measure of strain, which is plotted at the right in Figure 8. In this series of tests, the maximum strain extracted is slightly less than  $50 \mu\epsilon$  (microstrain). This calculation assumes that the surface wave speed does not change with strain, a condition that is not necessarily correct for all piezoelectric materials. However, it has been established [7] as a valid assumption for bulk lithium niobate, and therefore the delay in arrival time is a result only of elongation.

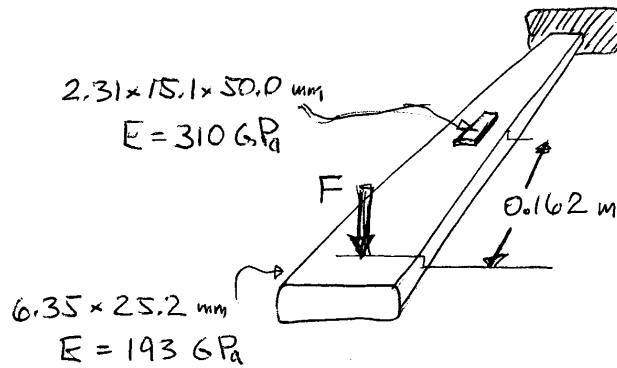


Figure 7. Test setup for strain sensing

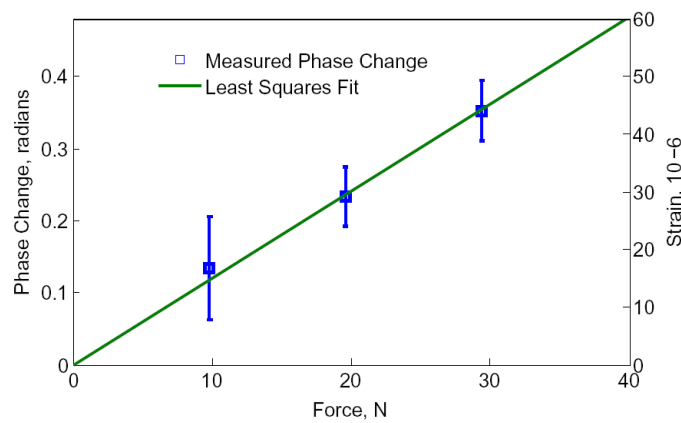


Figure 8. Measured phase difference (left) and strain (right) with increasing load

The data observed in Figure 8 is linear with increasing load, with an appropriate intercept at the origin. Other strain experiments performed directly on the package (not shown) demonstrated comparability, stability and repeatability under different levels of quasi-static loading. The standard deviation noted in Figure 8 corresponds to a strain increment of roughly  $4 \mu\epsilon$ , which is a high level of precision for structural strain monitoring. The typical strain under dead load in steel structures used for civil infrastructure, such as bridges, is roughly  $300 \mu\epsilon$ , and strain changes of interest during monitoring are likely to be several hundred  $\mu\epsilon$ . Therefore, the strain sensitivity and accuracy shown in Figure 8 are ample for the intended structural applications.

In our experimental configuration, the ceramic package provides a significant stiffening of the stainless steel specimen at the location where strain is being measured, and therefore our prediction (calculation) of strain must model the composite cross-section. Under those assumptions, the strain at the top fiber of the ceramic package is calculated to be  $70 \mu\epsilon$  under our maximum test load. Therefore, the strain measurement extracted from the SAW device is roughly 70% of that predicted strain, which is a reasonable discrepancy when we recognize that the SAW device is bonded with epoxy to the cavity inside of the ceramic package, and therefore experiences a strain less than that present at the top fiber.

However, there remains a significant concern regarding the need for temperature compensation. The change in surface acoustic wave speed with temperature for lithium niobate is 75 ppm/ $^{\circ}$ C. Therefore, a modest change in temperature will produce a phase difference (shift, delay) considerably greater than produced by the strain changes of interest. Accordingly, temperature compensation must be attained with high confidence for this strain measurement technology to be useful. As noted earlier [8], this condition was addressed in the development of a wireless pressure sensor, although its implementation for strain sensing remains a new research question.

## 6. PRELIMINARY TESTS OF WIRELESS OPERATION

In addition to devices fabricated on lithium niobate, in our recent research activities we have designed and fabricated SAW devices on quartz and on Langasite. In those research activities we also address wireless operation, and Figure 9 shows echoes returned in preliminary wireless experiments at distances of 30 and 50 cm. The wireless operation was configured with simple dipole antennae and not otherwise optimized, and the results are shown to demonstrate the fact that wireless, passively powered operation of SAW devices is realistic. As noted earlier, other researchers have discussed wireless operation at distances of 10 m when an antenna with high directionality is used at the scanner.

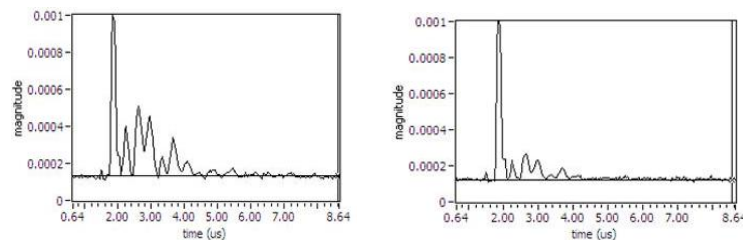


Figure 9. Typical reflections detected at excitation source, wireless operation at (left) 30 and (right) 50 cm

## 7. CONCLUSIONS

We summarize our recent experience with the design, fabrication, and testing of SAW devices. We show that a device fabricated on bulk lithium niobate can act as a sensitive and reasonably linear strain sensor, with a resolution that is sufficiently sensitive for applications of structural sensing and monitoring. However, we note that temperature compensation must be provided. We discuss demonstrations by others of passively powered wireless operation, and show preliminary results that we obtained in our laboratory on other devices showing effective operation in a wireless configuration.

## ACKNOWLEDGEMENTS

This work was performed in support of ongoing research in sensor systems and diagnostics at the National Energy Technology Laboratory under RDS contract DE-AC26-04NT41817. This technology is being studied in the course of the development of sensors for measurement of oxygen levels in advanced oxy-fuel powerplants that can capture CO<sub>2</sub>.

## REFERENCES

1. D. S. Ballantine et al., [Acoustic Wave Sensor: Theory, Design, and Physico-Chemical Applications], Academic Press (1997).
2. X. Q. Bao, W. Burkhard, V. V. Varadan, V. K. Varadan, "SAW Temperature Sensor and Remote Reading System," Proc. IEEE Ultrasonics Symposium, pp. 583-585, (1987).

3. W.-E. Bulst et al., "State of the art in wireless sensing with surface acoustic waves," *IEEE Trans. Ind. Elect.* 48, 265 (2001)
4. C. Campbell, [Surface Acoustic Wave Devices and Their Signal Processing Applications], Academic Press, (1989).
5. S. Datta, [Surface Acoustic Wave Devices], Prentice-Hall, (1985).
6. B. Dixon, V. Kalinin, J. Beckley, R. Lohr, "A Second Generation In-Car Tire Pressure Monitoring System Based on Wireless Passive SAW Sensors," *International Frequency Control Symposium and Exposition*, pp. 374-380 (2006).
7. A. L. Nalamwar, M. Epstein, "Strain Effects in SAW Devices," *Proc. IEEE* 64(5), pp. 613-615, (1976).
8. L. Reindl, *Wireless Passive SAW Identification Marks and Sensors*, Tutorial notes, *IEEE Ultrasonics Conference*, New Orleans, (2002).
9. R. Steindl et al., "SAW delay lines for wirelessly requestable conventional sensors," *Proc. IEEE Ultrasonics Symposium*, pp. 351-354, (1998).
10. R. Steindl et al., "Wireless magnetic field sensor employing SAW-transponder," *Proc. IEEE International Symposium on Applications of Ferroelectrics*, pp. 855-858, (2000).
11. V. V. Varadan, V. K. Varadan, X. Bao, S. Ramanathan, and D. Piscotty, "Wireless passive IDT strain microsensor," *Smart. Mater. Struct.* 6, pp. 745-751, (1997).
12. R. White, F. Voltmer, "Direct piezoelectric coupling to surface elastic waves," *Appl. Phys. Ltrs.* (7), pp. 314-316, (1971).
13. U. Wolff et al., "Radio accessible SAW sensors for simultaneous non-contact measurement of torque and temperature," *Proc. IEEE Ultrasonics Symp.*, pp. 359-362, (1996).